ORIGINAL ARTICLE

Machine Learning for Multi-Vessel Coronary Artery Disease Prediction on Electrocardiogram Gated Single-Photon Emission Computed Tomography

Masato Shimizu, MD[1)], Shigeki Kimura, MD[1)], Hiroyuki Fujii, MD[1)], Makoto Suzuki, MD[1)], Mitsuhiro Nishizaki, MD[2)], and Tetsuo Sasano, MD[3)]

Received: April 25, 2022/Revised manuscript received: August 8, 2022/Accepted: August 15, 2022
J-STAGE advance published: September 29, 2022

Abstract

***Background*: Single-photon emission computed tomography (SPECT) encounters difficulties in diagnosing severe multi-vessel coronary artery disease (svMVD) because of balanced ischemia. We estimated the predictive value of electrocardiogram-gated SPECT for svMVD and improved it using machine learning (ML).**

***Methods and results*: We enrolled consecutive 335 patients (median age, 74 years; 255 men) who underwent adenosine stress-gated SPECT (^{99m}Technesium) and coronary angiography. svMVD was defined as three-vessel disease or left main tract stenosis. Predictive models were constructed using statistical and ML methods. Eighteen cases (5%) showed svMVD, and diabetes, summed stress score (SSS), and the max difference among segmental time of stroke volume per cardiac cycle (MDSV: a parameter of left ventricular [LV] end-systolic dyssynchrony) on adenosine stress were independent significant predictors. The area under the receiver operating characteristic curve (AUC) of SSS and MDSV on stress were 0.759 and 0.763, respectively. Conversely, the extra trees classifier and light gradient boosting machine had improved AUC values of 0.826 and 0.870, respectively, and the MDSV on stress and diabetes showed high feature values in the ML models.**

***Conclusion*: ML on SPECT helped to improve the diagnostic performance of svMVD and diabetes, and the parameters of LV dyssynchrony played essential roles in the ML predictive models.**

Keywords: Max difference among segmental time of stroke volume per cardiac cycle, Machine learning, Multi-vessel coronary artery disease, SHapley Additive exPlanation method, Single-photon emission computed tomography

Ann Nucl Cardiol 2023; 9 (1): 11–18

Multi-vessel coronary artery disease (MVD) has been recognized to be serious heart disease. Recently, percutaneous coronary artery intervention was reported to have no advantage to optimal medical therapy even for patients including MVD cases (1). However, the study excluded left main tract (LMT) lesion, and triple vessel disease is still considered to bring worse prognosis (2). Severe MVD (svMVD) defined as triple vessel disease and/or LMT lesion is considered as life threatening disease, and it is still inevitable to be treated by coronary re-vascularization.

Single-photon emission computed tomography (SPECT) is a common tool to evaluate myocardial ischemia. However, it has limited capability when considering patients diagnosed with MVD (3). The summed stress score (SSS) and summed difference score (SDS) are used to evaluate myocardial ischemia. However, the diagnostic performance is inadequate in MVD cases because of balanced ischemia (4). Several procedures have used SPECT for diagnosing MVD effectively. Transient ischemic dilatation (TID) of the left ventricle (LV), caused by stress, is a well-known predictor of MVD. Conventionally, the accuracy is reported to be low (5). The washout ratio of ^{201}Thallium-Chloride SPECT on stress is

DOI: 10.17996/anc.22-00155

1) Department of Cardiology, Yokohama Minami Kyosai Hospital, Yokohama, Japan
2) Odawara Cardiovascular Hospital, Odawara, Japan
3) Department of Cardiovascular Medicine, Tokyo Medical and Dental University, Tokyo, Japan

reported to be a predictor of MVD (6); however, its accuracy is limited, and it gives patients a higher exposure dose than ^{99m}Technesium (^{99m}Tc). Hida et al. reported that the LV dyssynchrony parameters of electrocardiography (ECG)-gated SPECT on stress were useful for evaluating MVD (7); however, few studies have evaluated this hypothesis.

Conversely, machine learning (ML) has been rapidly developed and applied to SPECT, to detect myocardial ischemia (8). Several ML models of SPECT have demonstrated a relatively high diagnostic performance (9, 10), but there are few studies that utilize ML for MVD; notably, there are no studies on the parameters of LV function and dyssynchrony.

This study evaluated the predictive value of ML on ECG-gated SPECT for svMVD and investigated the predictive value of LV dyssynchrony parameters.

Methods

Study patients

The inclusion criteria were patients aged >18 years who underwent both adenosine stress ECG-gated ^{99m}Tc SPECT and coronary angiography within 3 months at Yokohama Minami Kyosai Hospital. The exclusion criteria were as follows: patients having no sinus rhythm, with a history of surgical coronary artery bypass grafting, and whose images showed poor/small LV cavity (end-systolic volume ≤15 mL). From June 2013 to January 2022, we recruited consecutive 335 patients (median, 74.0 years [interquartile range (IQR): 68, 79], 255 men). The primary reasons for SPECT were as follows: chest pain in 117 patients, abnormal ECG in 40 patients, follow-up for ischemic heart diseases in 129 patients, congestive heart failure and low LV ejection fraction in 34 patients, and other causes in 15 patients. The median pre-test probability of coronary artery disease was 36% [IQR: 22%, 53%], which was estimated in the previous report (11). Positive criteria for svMVD was defined as three-vessel disease or left main tract stenosis, with an excluded side-branch stenosis having a more rigid definition than that described in a previous report (12). Positive coronary artery stenosis was defined with >75% stenosis and a positive fractional flow reserve (FFR) value of ≤0.80 (13). FFR was evaluated with a pressure wire by hyperaemia evoked following nicorandil infusion into the coronary artery, as previously described (13). The ethics committee of Yokohama Minami Kyosai Hospital approved the study protocol, and written informed consent was obtained from all participants prior to the study.

ECG-gated SPECT

The semiconductor cadmium zinc telluride (CZT)-based ultrafast cardiac camera system (Discovery NM 530c®; GE Medical Systems, Milwaukee, WI, USA) was utilized and operated on a Windows-based workstation (Xeleris® TM3; GE Medical Systems, Milwaukee, WI, USA); it can evaluate patients having high degree of wall motion abnormalities (14). The radioisotope dose of ^{99m}Tc was 740 MBq/person, and the images were acquired and reconstructed using a gamma-camera system with a multiple-pinhole collimator and 19 stationary CZT detectors, as previously described (15).

SPECT on stress was performed using adenosine injection (120 μg/kg/min) by stress first procedure, and with 3 hours interval between stress and rest. Myocardial perfusion was estimated using Heart Risk View-S® and LV function by Heart Risk View-F® (Nihon Medi-Physics Co., Ltd., Tokyo, Japan), based on the standard database of the Japanese Nuclear Cardiology Working Group 2007 (16). The gating frames per cardiac cycle were 16, and the LV time-volume curve was constructed to estimate the LV volumes and functions, which was previously described (17). Diastolic functions were assessed using peak filling rate. The summed rest score, SSS, and SDS were measured as myocardial perfusion, as previously reported (18).

LV dyssynchrony was estimated using a two-phase analysis method. The first was the onset analysis of LV contraction (Figure 1, left side). The distribution of the LV contraction onset was presented in a 360° polar map and in a phase histogram, and 95% of the width of the phase histogram (bandwidth) and the phase standard deviation (SD) were calculated. The second analysis was of the end-systole of the LV contraction (Figure 1, right side). From the time-volume curve of the LV 17 segments, the time from the beginning of the cardiac cycle to the end-systole was defined as the time to end-systole (TES). The SD of TES per cardiac cycle was defined as SD-TES (%), and the maximum difference among segmental time of stroke volume per cardiac cycle was defined as MDSV (%) (19). All parameters on adenosine stress had prefixes added: prefix ‘s’ (ex. ejection fraction [EF] on stress as sEF), and at rest prefix ‘r’ (ex. rEF).

Statistical analysis and predictive model construction by statistical procedures

Numeric variables are displayed as median values [IQR: 25% value, 75% value]. To compare the svMVD (+) and svMVD (-) groups, the Mann-Whitney test used numeric variables. Fisher’s exact test evaluated differences in categorical variables. All parameters were evaluated using univariate logistic regression analysis, and among the significant predictors, a pair of parameters having multicollinearity was extracted. Multicollinearity was defined as a correlation coefficient >0.90, and a parameter with a larger P value in univariate logistic regression was excluded. After the procedure, a multivariate logistic regression analysis (stepwise

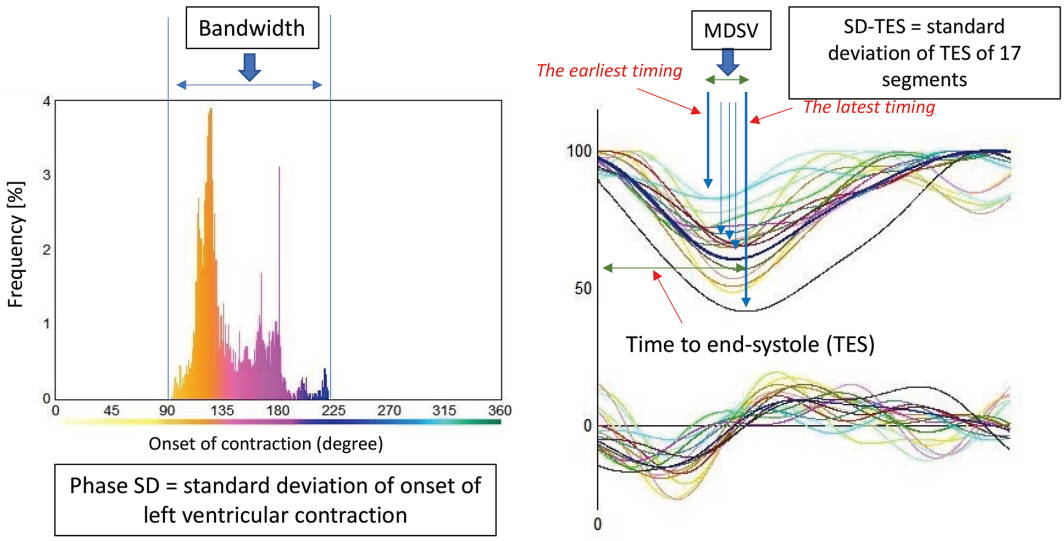

Figure 1 Two methods of estimating left ventricular dyssynchrony.
Left side figure: phase histogram of one cardiac cycle, which shows the onset timing of LV contraction. Bandwidth: 95% bandwidth of the histogram; phase SD: standard deviation of the histogram. Figure on the right side shows 17 segmental time-volume curves of one cardiac cycle, which shows the end-systolic timing of each segment (blue arrows).
SD-TES: standard deviation of time to end-systole of 17 segments, MDSV: maximum difference among segmental times of stroke volume (difference between the earliest and the latest end-systole in 17 segments).

regression) was performed, and significant independent predictors were estimated.

From the receiver operating characteristics (ROC) curve analysis of the independent predictors, the cut-off value that showed the highest specificity/sensitivity set was measured. The data over and below the cut-off value were considered positive and negative, respectively. The diagnostic performance of the predictors was evaluated and compared using a confusion matrix and Cramer's V analysis (20).

Statistical significance was set at $P<0.05$. All statistical analyses were performed using EZR (Saitama Medical Center, Jichi Medical University, Saitama, Japan), which is a graphical user interface for R (The R Foundation for Statistical Computing, Vienna, Austria) (21).

Predictive model construction by machine learning

As ML methods, we adopted two established ML models: an extra trees classifier (model_ET) (22), a light gradient boosting machine (model_LGBM) (23). These models were built using PyCaret, which is an open-source wrapper over several ML libraries in Python with a low-code environment (24). Eleven ML models were evaluated by PyCaret simultaneously, and the top two models with high area under ROC curve (AUC) were model_LGBM and model_ET. Input data was selected by univariate analysis for svMVD and prepared as csv form, and output data was 0 (no svMVD) or 1 (svMVD) which is diagnosed by probability was over and below 0.5. All data (335 cases) were randomly split into 70% (234 cases) training data and 30% (101 cases) validation data. Ten random predictions and validations were conducted. Because of the imbalanced dataset (small number of svMVD cases), we applied one of the oversampling methods, adaptive synthetic sampling (ADASYN), on the training data, as previously described (25).

To estimate the feature importance of the models, the SHapley Additive exPlanations (SHAP) method was introduced to train the data (26). The optimal Shapley values for a game are the basis of the SHAP method, and its summary plot combines feature importance with effects.

Results

Of the 335 cases, 18 (5%) showed severe MVD, and its breakdown is shown in Table 1. Table 2 presents a comparison between the svMVD (+) and svMVD (−) groups. Univariate logistic regression analysis extracted 15 significant predictors of the extracted data, which are marked with asterisks (*) on the P-values in Table 2. A multivariate analysis (stepwise regression) showed that diabetes (odds ratio: OR 23.8, P=0.004), SSS (OR, 1.10; P<0.001), and sMDSV (OR, 1.03; P=0.045) were significant and independent predictors. The ROC curve analysis showed that the AUCs of SSS and sMDSV were 0.759 and 0.763, respectively. Table 3 presents the performance results of the three predictors and ML predictive models. Because of the imbalanced dataset (only 5% svMVD cases), the diagnostic performance was not evaluated in terms of specificity and sensitivity but in terms of positive predictive value, sensitivity, and F1-score which were the harmonic means. The F1-score for diabetes, SSS, and sMDSV were low

Table 1　Breakdown of coronary artery disease

		Location	Number
No lesion 196 cases			
Lesion (+) 139 cases	Single vessel 91 cases	LAD alone	48
		RCA alone	29
		LCx alone	14
	Double vessel 30 cases	LAD+RCA	12
		LAD+LCx (excluding LMT)	12
		RCA+LCx	6
	svMVD 18 cases	Triple vessel disease (including LMT)	13
		LMT stenotis (excluding RCA stenosis)	5

Severe multi-vessel disease (svMVD) was defined as three-vessel disease or left main tract (LMT) stenosis.
LAD: left anterior descending, RCA: right coronary artery, LCx: left circumflex.

(0.186, 0.208, and 0.211, respectively). Conversely, the ML predictive models demonstrated higher AUCs and F1-scores than those of the three predictors. The AUCs of the ML models were 0.826 for model ET, 0.870 for model LGBM, and the F1-score were 0.500, and 0.429, respectively.

Figure 2 shows the SHAP values of the features on the models. The red point indicates svMVD (+) and the blue point svMVD (−) cases. The Shapley value of each feature is displayed on the x-axis, (defined as the SHAP value), in which a large (right side) value corresponds to a positive contribution to the model. In both models, the sMDSV and diabetes showed high feature values for building the models.

Discussion

We investigated the predictive value of ML for severe MVD and found that MDSV was an excellent predictor of stress, similar to SSS. The three ML models improved the diagnostic performance of statistical predictors. In the ML models, sMDSV demonstrated high feature importance as well as SHAP value, which is a novel method of explainable artificial intelligence (xAI).

Left ventricular dyssynchrony and multi-vessel disease

As the myocardial perfusion score on SPECT is evaluated by comparing each segment with a healthy segment, the score and polar map expression tend to be normal in MVD patients. Hida et al. reported that the degree of LV dyssynchrony of the onset of contraction predicted MVD, and they described a possible theory (7): LV dyssynchrony was induced by two different mechanisms: a temporal delay and contractile disparity. In the case of MVD, the LV contraction onset becomes random and reveals contractile disparity. However, with respect to the temporal delay of LV wall contraction, the end-systolic timing is substantially superior to the conventional parameters of contraction onset, such as phase SD and bandwidth. The evaluation of LV dyssynchrony on SPECT, which utilized the onset of contraction, was first reported in 2005 (27). The method of LV end-systolic timing is simple and estimated with a time-volume curve of 17 segments, which was first demonstrated in 2009 (28). Although the end-systolic method is easily measured, the onset method has been developed and applied. Conversely, the end-systolic method is the main and well-studied method in ultrasound echocardiography (UCG). Li et al. made time-volume curve by UCG and evaluated LV dyssynchrony by disparity of timing of end-systole (29). From the analysis, they concluded that LV dyssynchrony was associated with high Gensini scores, which indicated the presence of complex coronary artery stenosis. Lee et al. reported that even in patients with normal LV EF, mechanical dyssynchrony occurred in patients with coronary artery disease, without prior myocardial infarction and narrow QRS complexes (30). Patients diagnosed with svMVD as well as only heart failure patients with wide QRS should be evaluated with LV dyssynchrony, especially with MDSV.

Machine learning and myocardial ischemia

Several ML models have been reported for predicting coronary artery stenosis using SPECT. Guner et al. reported that utilizing myocardial perfusion image data and ML (a neural network), the presence of coronary artery disease could be diagnosed with high AUC (0.74), similar to that of an expert physician (0.84) (31). Arsanjani et al. demonstrated that a boosted ensemble was capable of diagnosing coronary artery disease with high accuracy (0.757) using only the total perfusion deficit score and TID data (9). Recently, a few reviews have been published on ML and cardiac imaging were published (8), but there are few studies on SPECT and coronary artery disease: there is no report on analysing LV functional parameters, including parameters of LV dyssynchrony.

Table 2 Comparison of two groups and logistic regression for severe multi-vessel disease

	svMVD (+) (N=18)	svMVD (-) (N=317)	Univariate			Multivariate		
			OR	95%CI	P	OR	95%CI	P
Age (y)	72 [66, 77]	74 [68, 79]	0.967	0.92-1.01	0.146			
Male (N, %)	16 (89%)	239 (75%)	2.610	0.59-11.6	0.207			
HTN (N, %)	12 (67%)	240 (76%)	0.642	0.23-1.77	0.391			
HL (N, %)	16 (89%)	207 (65%)	4.250	0.96-18.8	0.057			
DM (N, %)	17 (94%)	148 (47%)	19.400	2.55-148	0.004*	23.8	2.83-200	0.004
CKD (N, %)	6 (33%)	85 (27%)	1.360	0.50-3.75	0.547			
MI history (N, %)	6 (33%)	66 (21%)	1.900	0.69-5.26	0.215			
rHR (bpm)	78.8 [67.5, 84.0]	69.0 [62.0, 77.0]	1.040	1.00-1.08	0.029*			
rEDV (mL)	105.2 [79.2, 133.5]	87.0 [71.6, 110.5]	1.010	1.00-1.02	0.028*	NA		
rESV (mL)	50.3 [28.5, 68.2]	29.2 [20.9, 45.9]	1.010	1.00-1.03	0.009*	NA		
rEF (%)	54.2 [47.0, 64.1]	65.6 [56.6, 71.9]	0.952	0.92-0.99	0.005*			
rPFR (EDV/sec)	2.2 [1.4, 2.9]	2.1 [1.7, 2.6]	0.856	0.53-1.72	0.662			
rBandwidth (degree)	60 [42, 74]	38 [27, 54]	1.020	1.01-1.04	<0.001			
rPhase SD (degree)	16.6 [10.9, 24.0]	10.1 [7.2, 15.0]	1.070	1.03-1.12	0.001*	NA		
rMDSV (%)	13.3 [10.1, 21.5]	11.9 [8.9, 16.9]	1.020	0.98-1.06	0.427			
rSD-TES (%)	3.95 [2.77, 5.66]	3.34 [2.41, 4.66]	1.130	0.96-1.33	0.147			
sHR (bpm)	72.5 [67.0, 80.8]	68.0 [61.0, 75.0]	1.030	1.00-1.07	0.039*			
sEDV (mL)	112.1 [82.6, 142.9]	87.2 [72.3, 112.2]	1.010	1.00-1.02	0.028*			
sESV (mL)	54.0 [31.9, 74.7]	30.2 [21.6, 48.3]	1.020	1.00-1.03	0.005*			
sEF (%)	51.0 [46.9, 61.2]	64.5 [55.3, 70.8]	0.939	0.90-0.98	0.001*	NA		
sPFR (EDV/sec)	1.6 [1.1, 2.4]	2.1 [1.6, 2.5]	0.563	0.27-1.18	0.129			
sBandwidth (degree)	79.5 [62.5, 116.8]	53.0 [39.0, 76.0]	1.020	1.01-1.04	<0.001*			
sPhase SD (degree)	22.2 [17.6, 34.3]	14.7 [10.3, 21.5]	1.050	1.02-1.09	0.002*	NA		
sMDSV (%)	26.0 [16.9, 31.5]	12.7 [8.8, 19.3]	1.050	1.02-1.08	<0.001*	1.030	1.00-1.06	0.045
sSD-TES (%)	6.7 [4.3, 8.5]	3.5 [2.4, 4.9]	1.210	1.09--1.35	<0.001*	NA		
TID	0.99 [0.94, 1.09]	1.00 [0.96, 1.06]	0.548	0.005-62.3	0.804			
SRS	14 [6, 26]	8 [5, 14]	1.090	1.04-1.15	0.001*			
SSS	19 [13, 25]	10 [5, 15]	1.100	1.05-1.15	<0.001	1.100	1.04-1.17	<0.001
SDS	4 [1, 7]	1 [0, 4]	1.070	0.99-1.17	0.096			

Explanation of all parameters on adenosine stress had prefix ‘s’ added (ex. ejection fraction (EF) on stress as sEF), and at rest prefix ‘r’ (ex. rEF).
svMVD: severe multi-vessel disease, HTN: hypertension, HL: hyperlipidemia, DM: diabetes mellitus, CKD: chronic kidney disease, MI history: previous history of myocardial infarction, SRS/SSS/SDS: summed rest score/summed stress score/summed difference score in 17 segmental models, HR: heart rate (bpm: beats per minute), EDV: end-diastolic volume, ESV: end-systolic volume, EF: ejection fraction, PFR: peak filling rate, TID: transient ischemic dilatation (ratio of sEDV and rEDV), OR: odds ratio, 95%CI: 95% confidence interval, and other abbreviations are explained in Figure 1 legend.
P-values are the results of the univariate logistic regression. Non-applicable (NA) parameters were excluded because of multicollinearity in the multivariate analysis. Statistical significance was set at $p<0.05$.

Model_ET is an ensemble learning method that is composed of a large number of decision trees, and the method to divide trees is not the best fit but a random choice of the Gini coefficient or entropy (22). As a result, model_ET can maintain a high performance in the presence of noisy features, and it is advantageous when the importance of each variable is relatively low. In the present study, all predictors were significant, but their importance for svMVD was limited; model_ET was suitable for constructing a good predictive model.

Model_LGBM shows excellent diagnostic performance on table data (23). The model adopts the boosting method, a series data composition instead of bagging (bootstrap aggregating; used in the random forest method). The learning speed is faster than that of the parallel data composition of bagging. The decision tree of the model is a leaf-wise tree growth method that is much faster than the level-wise tree growth method (used in ex. XG boosting). Moreover, various hyperparameter tunings can be performed in the model. As a result, model_LGBM is advantageous if the number of

Table 3 Predictive models for severe multi-vessel disease

	AUC	95%CI of AUC
sMDSV	0.763	0.649-0.878
SSS	0.759	0.649-0.869
Light gradient boosting machine	0.87	0.839-0.902
Extra trees classifier	0.826	0.802-0.850

	ACC	Recall	Precision	F1-score	95%CI of F1	Log loss	Cramer's V
DM	0.555	0.533	0.103	0.186	NA	NA	0.201
sMDSV ≥16	0.666	0.656	0.121	0.211	NA	NA	0.418
SSS ≥14	0.704	0.703	0.121	0.208	NA	NA	0.495
Light gradient boosting machine	0.921	0.500	0.375	0.429	0.372-0.486	2.653	NA
Extra trees classifier	0.941	0.500	0.500	0.500	0.431-0.569	2.065	NA

AUC: area under receiver operating characteristics (ROC) curve analysis, 95%CI: 95% confidence interval, ACC: accuracy, Recall: sensitivity of the model, Precision: positive predictive value, F1-score: harmonic mean of recall and precision, sMDSV: maximum difference among segmental time of stroke volume (difference between the earliest and the latest timing of end-systole in 17 segments) on stress, DM: diabetes, SSS: summed stress score.
95%CI of F1 score was utilized to evaluate variability obtained from the 10-times machine learning trials. Log loss was calculated from the 10 times trial on ML models. Cramer's V was calculated to estimate importance of statistical models for predicting severe multi-vessel disease.

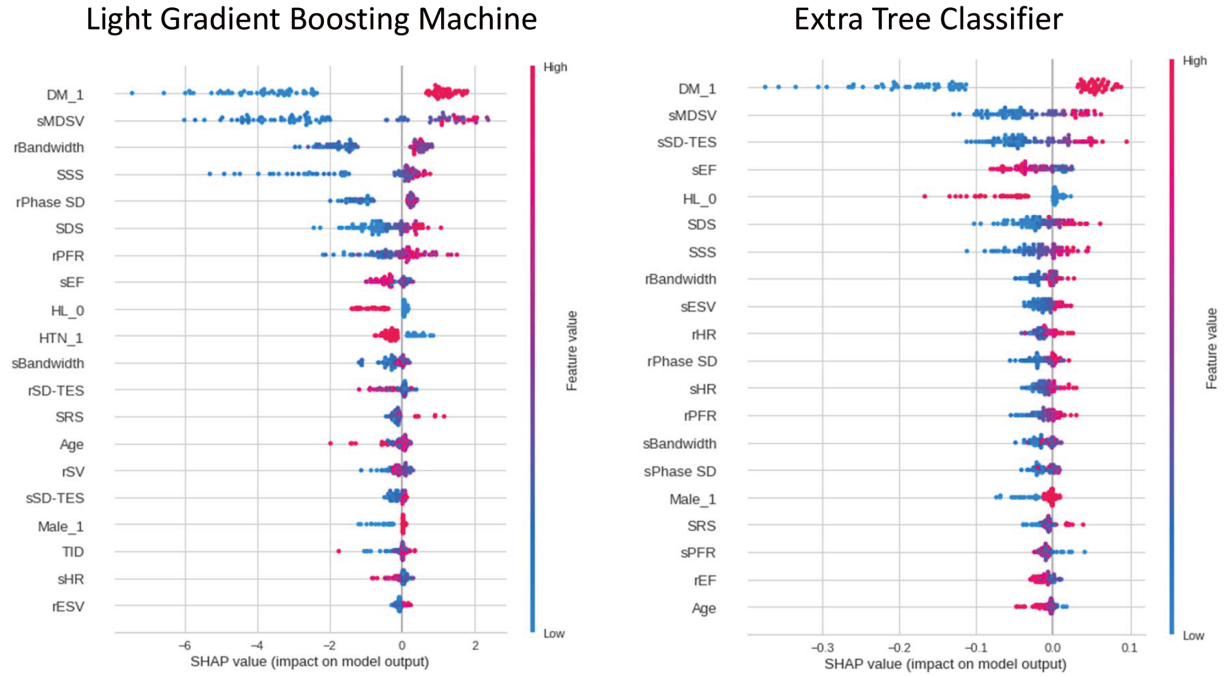

Figure 2 Interpretation of Feature importance on ML models.
Interpretation of Feature importance by SHapley Additive exPlanation (SHAP) method on two ML models. Left side: Plot of light gradient boosting machine, Right side: Plot of extra trees classifier. Each point on the summary plot corresponds to a SHAP value for a feature and an instance. Red point shows each case with severe multi-vessel disease (svMVD), and blue point shows no svMVD case. On y-axis, features were sorted according to their importance; colour shows the feature value from low (blue) to high (red). On the x-axis, the SHAP value was displayed, in which left side (minus value) shows negative and right side (plus value) positive impact. Abbreviations are explained in Figure 1 legends, Table 2 footnote.

parameters is high and the importance for each is low, as in the present study.

Study limitations

The sample size of svMVD was small, therefore we could not set triple datasets (train-validation-test data). Because of the lack of the external test data, we could not compare statistical and ML models exactly, the possibility of overfitting was not sufficiently excluded, and external validity of the ML models was not robust. The pre-test probability of coronary

artery disease in the present study was higher than that in the general population (9). Therefore, our ML predictive model may be less applicable to the common population. Although the ML predictive models demonstrated high AUC, F1-score was relatively low. To improve F1-score, we might limit our study population to patients without a history of myocardial infarction. A cadmium-zinc-telluride gamma camera was used in the present study, but the system was not common. We did not adopt deep learning (neural network) as an ML model because of its unstable reproducibility and overfitting to training data. However, the use of deep learning models is inevitable, and their application in svMVD prediction is desirable.

Conclusions

ML on ECG-gated SPECT for severe MVD had a high diagnostic performance compared with conventional statistical prediction. Although the F1-score of ML models was not so high because we could not exclude the cases with myocardial infarction and heart failure, the AUC of ML models showed higher than that of conventional statistical predictors. The degree of end-systolic LV dyssynchrony on adenosine stress, which was measured by ECG-gated SPECT, played an essential role in building the ML models.

Acknowledgments

We thank Mr. Masami Hasegawa, Mr. Shigenori Uchida, and Mr. Kouji Hirabayashi for their technical assistance.

Sources of funding

None.

Conflicts of interest

The authors have no conflicts of interest to declare.

Abbreviation

MDSV: Max difference among segmental time of stroke volume per cardiac cycle
ML: Machine learning
MVD: Multi-vessel coronary artery disease
SHAP: SHapley Additive exPlanation method
SPECT: Single-photon emission computed tomography
SSS: Summed stress score

Reprint requests and correspondence:
Masato Shimizu, MD
Yokohama Minami Kyosai Hospital, 1-21-1 Mutsuura-higashi, Kanazawa-ku, Yokohama 236-0037 Japan
E-mail: mst-smz@my.email.ne.jp

References

1. Maron DJ, Hochman JS, Reynolds HR, Bangalore S, O'Brien SM, Boden WE, et al. Initial invasive or conservative strategy for stable coronary disease. N Engl J Med 382; 15: 1395–407.
2. Mohr FW, Morice MC, Kappetein AP, Feldman TE, Ståhle E, Colombo A, et al. Coronary artery bypass graft surgery versus percutaneous coronary intervention in patients with three-vessel disease and left main coronary disease: 5-year follow-up of the randomised, clinical SYNTAX trial. Lancet 2013; 381; 629–38.
3. Lima RSL, Watson DD, Goode AR, Siadaty MS, Ragosta M, Beller GA, et al. Incremental value of combined perfusion and function over perfusion alone by gated SPECT myocardial perfusion imaging for detection of severe three-vessel coronary artery disease. J Am Coll Cardiol 2003; 42: 64–70.
4. Sabharwal N, Lahiri A. Multi-vessel disease and CZT SPECT. Comparison with coronary angiography. J Nucl Cardiol 2017; 24: 696–7.
5. Driessen RS, Raijmakers PG, Danad I, Stuijfzand WJ, Schumacher SP, Lammertsma AA, et al. Adenosine single-photon emission computed tomography-derived transient ischemic dilatation and ejection fraction reserve fail to predict multivessel coronary artery disease. Nucl Med Commun 2019; 40: 773–4.
6. Bateman TM, Maddahi J, Gray RJ, Murphy FL, Garcia EV, Conklin CM, et al. Diffuse slow washout of myocardial thallium-201: A new scintigraphic indicator of extensive coronary artery disease. J Am Coll Cardiol 1984; 4: 55–64.
7. Hida S, Chikamori T, Tanaka H, Igarashi Y, Shiba C, Usui Y, et al. Diagnostic value of left ventricular dyssynchrony after exercise and at rest in the detection of multivessel coronary artery disease on single-photon emission computed tomography. Circ J 2012; 76: 1942–52.
8. Al'Aref SJ, Anchouche K, Singh G, Slomka PJ, Kolli KK, Kumar A, et al. Clinical applications of machine learning in cardiovascular disease and its relevance to cardiac imaging. Eur Heart J 2019; 40: 1975–86.
9. Arsanjani R, Xu Y, Dey D, Vahistha V, Shalev A, Nakanishi R, et al. Improved accuracy of myocardial perfusion SPECT for detection of coronary artery disease by machine learning in a large population. J Nucl Cardiol 2013; 20: 553–62.
10. Arsanjani R, Dey D, Khachatryan T, Shalev A, Hayes SW, Fish M, et al. Prediction of revascularization after myocardial perfusion SPECT by machine learning in a large population. J Nucl Cardiol 2015; 22: 877–84.
11. Genders TSS, Steyerberg EW, Alkadhi H, Leschka S, Desbiolles L, Nieman K, et al. A clinical prediction rule for the diagnosis of coronary artery disease: validation, updating, and extension. Eur Heart J 2011; 32: 1316–30.
12. Bryer E, Stein E, Goldberg S. Multivessel coronary artery disease: The limitations of a "one-size-fits-all" approach. Mayo Clin Proc Innov Qual Outcomes 2020; 4: 638–41.
13. Pijls NHJ, Fearon WF, Tonino PAL, Siebert U, Ikeno F, Bornschein B, et al. Fractional flow reserve versus angiography for guiding percutaneous coronary intervention in patients with multivessel coronary artery disease: 2-year follow-up of the FAME (Fractional Flow Reserve Versus Angiography for Multivessel Evaluation) study. J Am Coll Cardiol 2010; 56:

177–84.
14. Bailliez A, Blaire T, Mouquet F, Legghe R, Etienne B, Legallois D, et al. Segmental and global left ventricular function assessment using gated SPECT with a semiconductor Cadmium Zinc Telluride (CZT) camera: Phantom study and clinical validation vs cardiac magnetic resonance. J Nucl Cardiol 2014; 21: 712–22.
15. Kano N, Okumura T, Isobe S, Sawamura A, Watanabe N, Fukaya K, et al. Left ventricular phase entropy: Novel prognostic predictor in patients with dilated cardiomyopathy and narrow QRS. J Nucl Cardiol 2018; 25: 1677–87.
16. Chono T, Onoguchi M, Shibutani T, Hashimoto A, Nakata T, Yama N, et al. Improvement in automated quantitation of myocardial perfusion abnormality by using iterative reconstruction image in combination with resolution recovery, attenuation and scatter corrections for the detection of coronary artery disease. Ann Nucl Med 2017; 31: 181–9.
17. Nakae I, Hayashi H, Matsumoto T, Mitsunami K, Horie M. Clinical usefulness of a novel program “Heart Function View” for evaluating cardiac function from gated myocardial perfusion SPECT. Ann Nucl Med 2014; 28: 812–23.
18. Berman DS, Abidov A, Kang X, Hayes SW, Friedman JD, Sciammarella MG, et al. Prognostic validation of a 17-segment score derived from a 20-segment score for myocardial perfusion SPECT interpretation. J Nucl Cardiol 2004; 11: 414–23.
19. Yamamoto A, Hosoya T, Takahashi N, Iwahara S, Munakata K. Quantification of left ventricular regional functions using ECG-gated myocardial perfusion SPECT—Validation of left ventricular systolic functions—. Ann Nucl Med 2006; 20: 449–56.
20. McHugh ML. The chi-square test of independence. Biochem Med (Zagreb) 2013; 23: 143–9.
21. Kanda Y. Investigation of the freely available easy-to-use software ‘EZR’ for medical statistics. Bone Marrow Transplant 2013; 48: 452–8.
22. Marée R, Geurts P, Wehenkel L. Random subwindows and extremely randomized trees for image classification in cell biology. BMC Cell Biol 2007; 8 Suppl 1: S2.
23. Ghiasi MM, Zendehboudi S. Application of decision tree-based ensemble learning in the classification of breast cancer. Comput Biol Med 2021; 128: 104089.
24. Gain U, Hotti V. Low-code autoML-augmented data pipeline – A review and experiments. J Phys: Conf Ser 2021; 1828: 012015.
25. Fotouhi S, Asadi S, Kattan MW. A comprehensive data level analysis for cancer diagnosis on imbalanced data. J Biomed Inform 2019; 90: 103089.
26. Lundberg S, Lee SI. A unified approach to interpreting model predictions. Advances in Neural Information Processing Systems. 2017. https://arxiv.org/abs/1705.07874
27. Chen J, Garcia EV, Folks RD, Cooke CD, Faber TL, Tauxe EL, et al. Onset of left ventricular mechanical contraction as determined by phase analysis of ECG-gated myocardial perfusion SPECT imaging: Development of a diagnostic tool for assessment of cardiac mechanical dyssynchrony. J Nucl Cardiol 2005; 12: 687–95.
28. Keida T, Ohira H, Fujita M, Chinen T, Nakamura K, Kato T, et al. Quantitative assessment of dyssynchrony using ECG-gated SPECT myocardial perfusion imaging prior to and following cardiac resynchronization therapy. Circ J 2009; 73: 1550–3.
29. Li M, Li L, Wu W, Ran H, Zhang P. Left ventricular dyssynchrony in coronary artery disease patients without regional wall-motion abnormality: Correlation with Gensini score. Echocardiography 2019; 36: 1689–97.
30. Lee PW, Zhang Q, Yip GW-K, Wu L, Lam YY, Wu EB, et al. Left ventricular systolic and diastolic dyssynchrony in coronary artery disease with preserved ejection fraction. Clin Sci (Lond) 2009; 116: 521–9.
31. Guner LA, Karabacak NI, Akdemir OU, Karagoz PS, Kocaman SA, Cengel A, et al. An open-source framework of neural networks for diagnosis of coronary artery disease from myocardial perfusion SPECT. J Nucl Cardiol 2010; 17: 405–13.